Differential Spatial Modulation Mapping Algorithms

WANG Chanfei, CHAI Jianxin, XU Yamei

(College of Computer and Communication, Lanzhou University of Technology, Lanzhou 730050, China)

DOI: 10.12142/ZTECOM.202403014

https://kns.cnki.net/kcms/detail/34.1294.TN.20240903.1032.004.html, published online September 3, 2024

Manuscript received: 2024-08-04

Abstract: Differential spatial modulation (DSM) is a multiple-input multiple-output (MIMO) transmission scheme. It has attracted extensive research interest due to its ability to transmit additional data without increasing any radio frequency chain. In this paper, DSM is investigated using two mapping algorithms: Look-Up Table Order (LUTO) and Permutation Method (PM). Then, the bit error rate (BER) performance and complexity of the two mapping algorithms in various antennas and modulation methods are verified by simulation experiments. The results show that PM has a lower BER than the LUTO mapping algorithm, and the latter has lower complexity than the former.

Keywords: spatial modulation (SM); multiple-input multiple-output (MIMO); Look-Up Table Order (LUTO); Permutation Method (PM); mapping algorithm

Citation (Format 1): WANG C F, CHAI J X, XU Y M. Differential spatial modulation mapping algorithms [J]. ZTE Communications, 2024, 22 (3): 116 – 122. DOI: 10.12142/ZTECOM.202403014

Citation (Format 2): C. F. Wang, J. X. Chai, and Y. M. Xu, "Differential spatial modulation mapping algorithms," *ZTE Communications*, vol. 22, no. 3, pp. 116 – 122, Sept. 2024. doi: 10.12142/ZTECOM.202403014.

1 Introduction

In order to enhance the transmission rate of wireless communications, various multi-antenna technologies have been proposed, among which spatial modulation (SM) technology[1 – 2] has garnered widespread attention due to its innovative nature. As a novel digital modulation method, SM technology conveys additional information through the On/Off states of transmission antennas, achieving an effective balance between spectral efficiency and energy efficiency. This approach reduces the number of radio-frequency chains, thereby decreasing implementation costs, and finds extensive applications across various signal domains, such as frequency, time, code and angle domains. Recent comprehensive review papers[3 – 4] have thoroughly delineated the fundamental principles, system design variants, and performance enhancement strategies of SM, providing crucial insights for understanding and advancing this technology. Concurrently, index modulation multiple access (IMMA), envisioned as an advanced technique for future 6G communications, is considered a novel extension of the traditional non-orthogonal multiple access (NOMA). It enhances spectral efficiency and energy efficiency and optimizes system performance and massive connectivity capabilities. Relevant literature[5 – 7] has delved deeply into the basic principles of IMMA and investigated its potential applications in various fields such as vehicular networks, reconfigurable intelligent surface (RIS)-aided networks, cooperative networks, and secure networks. Moreover, recent studies[8 – 9] have explored the application of index modulation technology in new areas such as green Internet of things (IoT) and dual-hop OFDM relay systems, further highlighting its advantages in improving communication efficiency and performance. These developments not only underscore the significance of index modulation technology in modern wireless communication, but also pave new paths and provide perspectives for its future evolution.

Building on this progress, differential spatial modulation (DSM), an important advancement in spatial modulation techniques, has emerged to address challenges in high-speed channel streaming and complex channel estimation in SM[10]. DSM introduces differential modulation in the time domain[11], retaining the benefit of SM's single transmit antenna activation per time slot while effectively avoiding channel estimation[12]. In a DSM system, the focus is on differential mapping coding at the transmitter[13] and demodulation at the receiver[14], with current research primarily directed towards mapping algorithms for antenna activation sequences and the development of efficient detection algorithms at the receiver[15 – 17]. As the

This work is supported by the National Natural Science Foundation of China (NSFC) under Grant No. 62061024 and the Project of Gansu Province Science and Technology Department under Grant No. 22ZD6GA055.

number of transmit streams increases with the antennas and modulation sequences, the performance of the DSM system is impacted. To this end, a differential spatial modulation detector with low complexity has been proposed[18], and algebraic differential spatial modulation has been explored[19]. A new generalized DSM scheme improving data transmission rates through symbol interleaving techniques is introduced in Ref. [20]. For high mobility scenarios, a low-complexity detector that enhances performance in fast fading channels is proposed[21], alongside a reordered amplitude phase-shift keying-assisted DSM scheme and a low-complexity detection algorithm[22], significantly improving performance under fast fading conditions. Differing from previous studies, this paper focuses on the mapping algorithm of DSM[23], elaborating on the design of the activation sequence for the look-up table order (LUTO) and permutation method (PM) and further designing a mapping table for LUTO when the number of transmit antennas is large. Our simulation validates that, in terms of the bit error rate (BER), PM slightly outperforms LUTO, with the extended PM algorithm showing a slight improvement in system performance compared to existing literature[16]. Depending on system requirements, different mapping algorithms can be selected in practical applications.

The remainder of this paper is organized as follows. In Section 2, a brief review of a DSM system model is presented. Two mapping algorithms are described in Section 3 and complexity analysis is provided in Section 4. In Section 5, we present the simulation results. The conclusion is given in Section 6.

Notations are as follows: $(\cdot)^T$ and $\mathrm{Tr}(\cdot)$ denote the transpose and trace of the matrix, respectively; $\mathrm{Re}\{\cdot\}$ represents the real component of the argument; the complex number field is denoted with $\mathbb{C}$.

2 System Model

Consider a fundamental band DSM system with N_T transmit antennas and N_R receive antennas. At the transmitter, the information bits are divided into each of $\log_2\left(N_T!\right) + N_T \log_2(M)$ bits in a transmit block[4] and are transmitted on N_T time slots, where M denotes the modulation order. Note that in the DSM system, the transmitting antennas and the length of a transmitted block is N_T. At the time of transmission duration T, the transmission matrix $\boldsymbol{S}_T \in \mathbb{C}^{N_T \times N_T}$ is

$$\boldsymbol{S}_T = \boldsymbol{S}_{T-1}\boldsymbol{X}_T, \tag{1}$$

where $\boldsymbol{X}_T \in \mathbb{C}^{N_T \times N_T}$ is the message matrices. Let $\boldsymbol{H}_T \in \mathbb{C}^{N_R \times N_T}$ represent the channel matrix. Then the received signal matrix $\boldsymbol{Y}_T \in \mathbb{C}^{N_R \times N_T}$ can be expressed as

$$\boldsymbol{Y}_T = \boldsymbol{H}_T\boldsymbol{S}_T + N_T. \tag{2}$$

Assuming that the channel is a flat Rayleigh fading channel, we consider the channel is invariant between two consecutive transmissions[6], and then we have $\boldsymbol{H}_T = \boldsymbol{H}_{T-1}$. Therefore, Eq. (2) can be rewritten as

$$\boldsymbol{Y}_T = \boldsymbol{Y}_{T-1}\boldsymbol{X}_T - N_{T-1}\boldsymbol{X}_T + N_T. \tag{3}$$

The estimation of $\boldsymbol{X}_T$ based on the maximum likelihood (ML) rule can be expressed as

$$\hat{\boldsymbol{X}}_T = \underset{\forall X \in R_M}{\operatorname{argmin}} \left\| \boldsymbol{Y}_T - \boldsymbol{Y}_{T-1}\boldsymbol{X}_T \right\|_F^2. \tag{4}$$

Thus, the optimal detector can be derived as

$$\hat{\boldsymbol{X}}_T = \underset{\forall X \in R_M}{\operatorname{argmax}}\ \mathrm{Tr}\left\{\mathrm{Re}\left\{\boldsymbol{Y}_T^H\boldsymbol{Y}_{T-1}\boldsymbol{X}_T\right\}\right\}, \tag{5}$$

where R_M denotes the set consisting of all effective information matrices. At last, the information bits are recovered by demapping the estimated antenna activation order. In the following, the mapping algorithms will be formulated.

3 Mapping Algorithms

3.1 LUTO

The LUTO algorithm is an efficient mapping method for matching data symbols to antenna combinations. Specifically, the antenna indices are divided into groups; each group contains several antenna indices, and each bit is used to select a group. The antenna indices within each group are arranged in a certain order, and the order among different groups can be customized as needed. To summarize, the implementation steps of the algorithm are as follows:

Step 1: Predefine an antenna combination mapping table corresponding to each data symbol;

Step 2: Convert the entered data symbols to the desired antenna combination;

Step 3: Map the antenna combinations and transmit the data symbols.

The signal matrix $\boldsymbol{S}_{T+1}$ is calculated by Eq. (1). Examples of binary phase shift keying (BPSK) and differential transmission processes with N_T=3 are shown in Table 1.

Table 2 shows the mapping table for the LUTO algorithm when N_T=3. For further study, the matrix of all signals sent by the system is shown in Table 3 when the input bit stream is 00 with BPSK modulation. Normally, the number of table rows is $2^{\log_2\left(N_T!\right)}$, and the total number of the mapping schemes generated is $N_T!$. Therefore, part of mapping scheme would be dropped. The formula for discarding the number of mapping schemes can be expressed as

$$L = N_T! - 2^{\log_2\left(N_T!\right)}. \tag{6}$$

The table column is related to the modulation order, which is determined by the following steps.

Step 1: Generate the value of the bits to be entered;

▼**Table 1. Differential transmission in differential spatial modulation (DSM) with binary phase shift keying (BPSK) modulation and $N_T = 3$**

Index t	0	1	2	3
Time interval	0, 1, 2	3, 4, 5	6, 7, 8	9, 10, 11
Input bit	No information sent	01010	10100	11110
Map to X_t	No information sent	$\begin{bmatrix} -1 & & \\ & & -1 \\ & +1 & \end{bmatrix}$	$\begin{bmatrix} & +1 & \\ +1 & & \\ & & +1 \end{bmatrix}$	$\begin{bmatrix} & -1 & \\ & & +1 \\ +1 & & \end{bmatrix}$
Actual transmitted signal matrix S_t	$\begin{bmatrix} +1 & & \\ & +1 & \\ & & +1 \end{bmatrix}$	$\begin{bmatrix} -1 & & \\ & & -1 \\ & +1 & \end{bmatrix}$	$\begin{bmatrix} & -1 & \\ & & -1 \\ +1 & & \end{bmatrix}$	$\begin{bmatrix} & -1 & \\ & & -1 \\ -1 & & \end{bmatrix}$

▼**Table 2. Mapping table of LUTO algorithm when $N_T = 3$**

Input Bitstream	Antenna Activation Sequence	Block of Information to Send
00	(1, 2, 3)	$\begin{bmatrix} s_1 & & \\ & s_2 & \\ & & s_3 \end{bmatrix}$
01	(1, 3, 2)	$\begin{bmatrix} s_1 & & \\ & & s_2 \\ & s_3 & \end{bmatrix}$
10	(2, 1, 3)	$\begin{bmatrix} & s_1 & \\ s_2 & & \\ & & s_3 \end{bmatrix}$
11	(2, 3, 1)	$\begin{bmatrix} & s_1 & \\ & & s_2 \\ s_3 & & \end{bmatrix}$

▼ **Table 3. Matrix of all signals sent with binary phase shift keying (BPSK) modulation and $N_T = 3$ when input bit D is 00**

Input Bits	Time Interval 1		Time Interval 2		Time Interval 3		Transmitted Signal Matrix
	Antenna Index	Symbol	Antenna Index	Symbol	Antenna Index	Symbol	
00000	1	−1	2	−1	3	−1	$\begin{bmatrix} -1 & & \\ & -1 & \\ & & -1 \end{bmatrix}$
00001	1	−1	2	−1	3	+1	$\begin{bmatrix} -1 & & \\ & -1 & \\ & & +1 \end{bmatrix}$
00010	1	−1	2	+1	3	−1	$\begin{bmatrix} -1 & & \\ & +1 & \\ & & -1 \end{bmatrix}$
00011	1	−1	2	+1	3	+1	$\begin{bmatrix} -1 & & \\ & +1 & \\ & & +1 \end{bmatrix}$
00100	1	+1	2	+1	3	+1	$\begin{bmatrix} +1 & & \\ & +1 & \\ & & +1 \end{bmatrix}$
00101	1	+1	2	+1	3	−1	$\begin{bmatrix} +1 & & \\ & +1 & \\ & & -1 \end{bmatrix}$
00110	1	+1	2	−1	3	+1	$\begin{bmatrix} +1 & & \\ & -1 & \\ & & +1 \end{bmatrix}$
00111	1	+1	2	−1	3	−1	$\begin{bmatrix} +1 & & \\ & -1 & \\ & & -1 \end{bmatrix}$

Step 2: Derive the maximum binary number from the 0/1 bit sequence based on the input bit value;

Step 3: Convert the maximum binary number to a decimal number;

Step 4: Add one to the resulting decimal number to determine the size of the table column.

As shown in Tables 4 and 5, the antenna activation sequence is given when $N_T = 4$ and $N_T = 5$. When $N_T = 4$, there are $N_T! = 4! = 24$ antenna activation sequences. From Eq. (6), it can be seen that among the 24 antenna activation orders, there will be eight antenna selection options not selected. The last eight of all schemes are generally discarded. The selected mapping scheme is represented by the set $D = \{D_0, D_1, \cdots, D_{15}\}$={(1,2,3,4), (1,2,4,3), (1,3,2,4), (1,3,4,2), (1,4,2,3), (1,4,3,2), (2,1,3,4), (2,1,4,3), (2,3,1,4), (2,3,4,1), (2,4,1,3), (2,4,3,1), (3,1,2,4), (3,1,4,2), (3,2,1,4), (3,2,4,1)}. Based on the formula $N_T \log_2(M) = 4\log_2(2) = 4$, a four-bit sequence is obtained. Converting the largest sequence 1111 to decimal and adding one yields a table with 16 columns. Define that U represents the full modulation symbol mapping scheme. Then, a permutation combination is obtained as U={(−1,−1,−1,−1), (−1,−1,−1,+1), (−1,−1,+1,−1), (−1,+1,−1,−1), (+1,−1,−1,−1), (−1,−1,+1,+1), (−1,+1,−1,+1), (+1,−1,−1,+1), (−1,+1,+1,+1), (+1,+1,+1,+1), (+1,+1,+1,−1), (+1,+1,−1,+1), (+1,−1,+1,+1), (+1, +1, −1, −1), (+1, −1, +1, −1), (+1, −1, −1, −1)}. Set $D = \{D_0, D_1, \cdots, D_{63}\}$ =(1,2,3,4,5), (1,2,3,5,4), (1,2,4,3,5), (1,2,4,5,3), (1,2,5,3,4,), (1,2,5,4,3), (1,3,2,4,5), (1,3,2,5,4), (1,3,4,2,5), (1,3,4,5,2), (1,3,5,2,4), (1,3,5,4,2), (1,4,2,3,5), (1,4,2,5,3), (1,4,3,2,5), (1,4,3,5,2), (1,4,5,2,3), (1,4,5,3,2), (1,5,2,3,4), (1,5,2,4,3), (1,5,3,2,4), (1,5,3,4,2), (1,5,4,2,3), (1,5,4,3,2), (2,1,3,4,5), (2,1,3,4,5), (2,1,3,5,4), (2,1,4,3,5), (2,1,4,5,3), (2,1,5,3,4), (2,1,5,4,3), (2,3,1,4,5), (2,3,1,5,4), (2,3,4,1,5), (2,3,4,5,1), (2,3,5,1,4), (2,3,5,4,1), (2,4,1,3,5), (2,4,1,5,3), (2,4,3,1,5), (2,4,3,5,1), (2,4,5,1,3), (2,4,5,3,1), (2,5,1,3,4), (2,5,1,4,3), (2,5,3,1,4), (2,5,3,4,1), (2,5,4,1,3), (2,5,4,3,1), (3,1,2,4,5), (3,1,2,5,4), (3,1,4,2,5), (3,1,4,5,2), (3,1,5,4,2), (3,1,5,2,4), (3,2,1,4,5), (3,2,1,5,4), (3,2,4,1,5), (3,2,4,5,1), (3,2,5,2,4), (3,2,5,4,1), (3,4,2,1,5), (3,4,2,5,1), (3,4,5,1,2)}.

From Eq. (6), it can be seen that by bringing $N_T = 5$ into $5! - 2^{\log_2(5!)} = 56$, there are 56 antenna activation sequences that will not be selected. Set U is arranged in the same way as $N_T = 4$. For $N_T = 4, 5$, each information block carries 8 and 11 data bits in the BPSK scheme of LUTO, respectively. It can be seen that as N_T and M increase, the transmission efficiency

▼Table 4. All the signal schemes of Look-Up Table Order (LUTO) with binary phase shift keying (BPSK) modulation and $N_T = 4$

		U										
		U_0	U_1	U_2	U_3		U_6	U_7		U_{13}	U_{14}	U_{15}
D	D_0	00000000	00000001	00000010	00000011	⋯	00000110	00000111	⋯	00001101	00001110	00001111
	D_1	00010000	00010001	00010010	00010011	⋯	00010110	00010111	⋯	00011101	00011110	00011111
	D_2	00100000	00100001	00100010	00100011	⋯	00100110	00100111	⋯	00101101	00101110	00101111
	⋯	⋯	⋯	⋯	⋯	⋯	⋯	⋯	⋯	⋯	⋯	⋯
	D_6	01100000	01100001	01100010	01100011	⋯	01100110	01100111	⋯	01101101	01101110	01101111
	D_7	01110000	01110001	01110010	01110011	⋯	01110110	01110111	⋯	01111101	01111110	01111111
	⋯	⋯	⋯	⋯	⋯	⋯	⋯	⋯	⋯	⋯	⋯	⋯
	D_{13}	11000000	11000001	11000010	11000011	⋯	11000110	11000111	⋯	11001101	11001110	11001111
	D_{14}	11010000	11010001	11010010	11010011	⋯	11010110	11010111	⋯	11011101	11011110	11011111
	D_{15}	11110000	11110001	11110010	11110011	⋯	11110110	11110111	⋯	11111101	11111110	11111111

▼Table 5. All the signal schemes of Look-Up Table Order (LUTO) with binary phase shift keying (BPSK) modulation and $N_T = 5$

		U									
		U_0	U_1	U_2		U_{14}	U_{15}		U_{29}	U_{30}	U_{31}
D	D_0	00000000000	00000000001	00000000010	⋯	00000001110	00000001111	⋯	00000011101	00000011110	00000011111
	D_1	00000100000	00000100001	00000100010	⋯	00000101110	00000101111	⋯	00000111101	00000111110	00000111111
	D_2	00001000000	00001000001	00001000010	⋯	00001001110	00001001111	⋯	00001011101	00001011110	00001111111
	⋯	⋯	⋯	⋯	⋯	⋯	⋯	⋯	⋯	⋯	⋯
	D_{14}	00111000000	00111000001	00111000010	⋯	00111001110	00111001111	⋯	00111011101	00111011110	00111011111
	D_{15}	00111100000	00111100001	00111100010	⋯	00111101110	00111101111	⋯	00111111101	00111111110	00111111111
	⋯	⋯	⋯	⋯	⋯	⋯	⋯	⋯	⋯	⋯	⋯
	D_{30}	01111000000	01111000001	01111000010	⋯	01111001110	01111001111	⋯	01111011101	01111011110	01111011111
	D_{31}	01111100000	01111100001	01111100010	⋯	01111101110	01111101111	⋯	01111111101	01111111110	01111111111
	⋯	⋯	⋯	⋯	⋯	⋯	⋯	⋯	⋯	⋯	⋯
	D_{61}	11110100000	11110100001	11110100010	⋯	11110101110	11110101111	⋯	11110111101	11110111110	11110111111
	D_{62}	11111000000	11111000001	11111000010	⋯	11111001110	11111001111	⋯	11111011101	11111011110	11111011111
	D_{63}	11111100000	11111100001	11111100010	⋯	11111101110	11111101111	⋯	11111111101	11111111110	11111111111

increases. The table size is 16×16=256 when $N_T = 4$. When $N_T = 5$, the table size is 32×64=2 048. As the transmitting antennas increase by one, the size of the table increases by 1 792 cells. Specifically, the size of the table increases exponentially with the transmitting antennas.

3.2 Permutation Method

From the previous subsection, it can be seen that the LUTO is not applicable to the case where the number of transmitting antennas is large. Thus, PM is introduced. This method forms a point-to-point mapping by permuting the order of N_R numbers. First, an integer m is mapped into a sequence, $a^{(m)} = \left(a_1^{(m)},\cdots,a_N^{(m)}\right)$, which is a set of permutations $\left\{1,\cdots,N_R\right\}$. For N_R, $m \in \left[0, N_R! - 1\right]$ can be represented as a sequence $a^{(m)}$ of length N_R. In short, the algorithm is implemented as follows.

Step 1: The input sequence is converted to an integer m.

Step 2: Integer m is converted to the sequence $b^m = \left(b_1^m,\cdots,b_{N1}^m\right)$, and the conversion is shown as

$$m = b_1^m\left(N_R - 1\right)! + \cdots + b_{N_T}^m 0!. \tag{7}$$

Take the largest b_1^m satisfying $b_1^m\left(N_1 - 1\right) \leqslant n_1$, and continue to find b_2^m satisfying $b_2^m\left(N_T - 2\right)! \leqslant m - b_1^m\left(N_T - 1\right)!$. And then all the b^m elements are computed in turn.

Step 3: the factorial sequence b^m is mapped into the arrangement $a^{(m)}$. Here $\Theta = \left(1, 2,\cdots, N_R\right)$ is defined as an ordered list, its first element index is 0, and the formula for converting b^m to $a^{(m)}$ is shown as

$$\underset{1 \leqslant i \leqslant N_T}{a_i^m} = \Theta_{b_i^m}, \tag{8}$$

so that the element $\Theta_{h^{(m)}}$ will be removed from list 1, and then each element of $a^{(m)}$ is obtained in a recursive way.

4 Complexity Analysis

The experimental platform utilizes the Windows 10 operating system, the programming environment is MATLAB 2016, and the CPU employed is an Intel Core i9-13900. Specifically, these configurations are detailed in Table 6.

Table 7 compares the program running times of the PM al-

▼**Table 6. Configuration of the test host**

CPU Type	Core Count	Thread Count	Core Types	Performance-Core Frequency	RAM
Core i9-13900	24	32	Alder Lake (12-th generation)	2.00 GHz	32 GB

▼**Table 7. Performance test results**

Test Items	Program Running Time/s	Test Items	Program Running Time/s
PM BPSK N_T = 3 N_R = 1	6.76	LUTO BPSK N_T = 3 N_R = 1	4.47
PM BPSK N_T = 3 N_R = 2	112.95	LUTO BPSK N_T = 3 N_R = 2	30.45
PM BPSK N_T = 3 N_R = 3	213.68	LUTO BPSK N_T = 3 N_R = 3	67.37
PM QPSK N_T = 3 N_R = 1	15.01	LUTO QPSK N_T = 3 N_R = 1	5.47
PM QPSK N_T = 3 N_R = 2	363.52	LUTO QPSK N_T = 3 N_R = 2	46.82
PM QPSK N_T = 3 N_R = 3	816.58	LUTO QPSK N_T = 3 N_R = 3	89.67
PM 8PSK N_T = 3 N_R = 1	44.54	LUTO 8PSK N_T = 3 N_R = 1	11.59
PM 8PSK N_T = 3 N_R = 2	370.16	LUTO 8PSK N_T = 3 N_R = 2	41.83
PM 8PSK N_T = 3 N_R = 3	1 969.85	LUTO 8PSK N_T = 3 N_R = 3	375.57
PM BPSK N_T = 4 N_R = 1	24.26	LUTO BPSK N_T = 3 N_R = 1	20.51
PM BPSK N_T = 4 N_R = 2	472.79	LUTO BPSK N_T = 4 N_R = 2	249.37
PM BPSK N_T = 4 N_R = 3	962.76	LUTO BPSK N_T = 4 N_R = 3	334.52
PM BPSK N_T = 4 N_R = 4	1 145.05	LUTO BPSK N_T = 4 N_R = 4	481.76
PM QPSK N_T = 4 N_R = 1	249.45	LUTO QPSK N_T = 4 N_R = 1	173.50
PM 8PSK N_T = 4 N_R = 1	1 323.63	LUTO 8PSK N_T = 4 N_R = 1	625.83
PM BPSK N_T = 5 N_R = 1	127.07	LUTO BPSK N_T = 5 N_R = 1	96.36
PM QPSK N_T = 5 N_R = 1	1 981.00	LUTO QPSK N_T = 5 N_R = 1	896.64
PM 8PSK N_T = 5 N_R = 1	56 551.78	LUTO 8PSK N_T = 5 N_R = 1	15 637.95

8PSK: 8 Phase shift keying
BPSK: binary phase shift keying
LUTO: Look-Up Table Order
PM: Permutation Method
QPSK: quadrature phase shift keying

gorithm and the LUTO algorithm under different conditions. From the table, it is evident that the LUTO algorithm outperforms the PM algorithm in terms of running time. This advantage becomes more pronounced as the number of antennas and the level of modulation order increase. This is because when the number of transmitting antennas is small, the LUTO algorithm does not incur any additional time complexity. However, as the number of antennas grows, the space complexity required by the LUTO algorithm increases exponentially. The PM algorithm, which converts the input bit stream into a signal matrix without using lookup tables, significantly reduces spatial complexity.

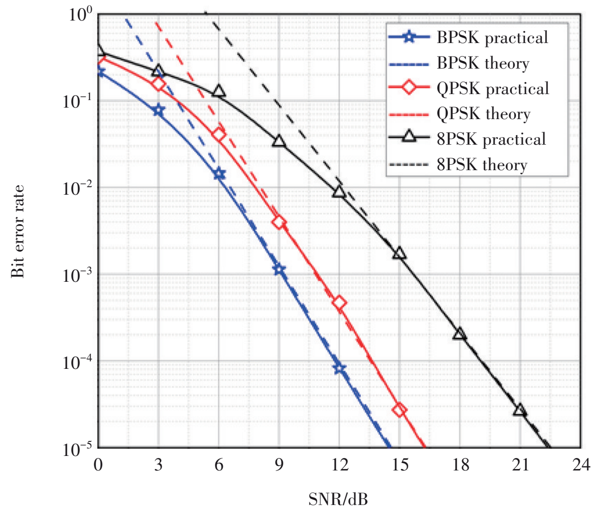

8PSK: 8 Phase shift keying
BPSK: binary phase shift keying
QPSK: quadrature phase shift keying
SNR: signal-to-noise ratio

▲**Figure 1. Simulation and theoretical results of Look-Up Table Order (LUTO) with N_T = 4 and N_R = 4**

5 Simulation Results and Discussion

In this section, we simulate and evaluate the BER performance of the DSM. The quasi-static Rayleigh flat fading channel is used in the experiments.

Fig. 1 gives the theoretical and simulation results of the LUTO for BPSK, QPSK and 8PSK modulation in DSM systems. It shows the performance of the DSM system when N_T = 4 and N_R=4. It can be seen that the higher the order of symbol modulation, the higher the data rate of the DSM system transmits.

Fig. 2 gives the comparative results of BER performance of DSM with N_T = 4, 5 and N_R=1, 2, 3, 4, 5 for PM and LUTO under BPSK modulation. At BER=10^{-1}, it can be seen that the SNR gain of the PM is slightly better than that of the LUTO for N_R = 1,N_T = 4 and N_T = 5. As the number of receiving antennas increases, the SNR gain of the PM gradually increases. The simulations show that the system performance is affected by the number of transmitting antennas. As the transmitting antenna number increases, the diversity gain increases.

Fig. 3 gives the BER performance of PM and LUTO in DSM with different modulations for N_T = 3, 4, 5, N_R = 3. When N_T = 4, there is roughly a 5.9 dB SNR loss at BER=10^{-3} for 8PSK compared to QPSK modulation. When N_T = 5, there is roughly 2.4 dB SNR loss for QPSK modulation compared to BPSK modulation at BER = 10^{-3}.

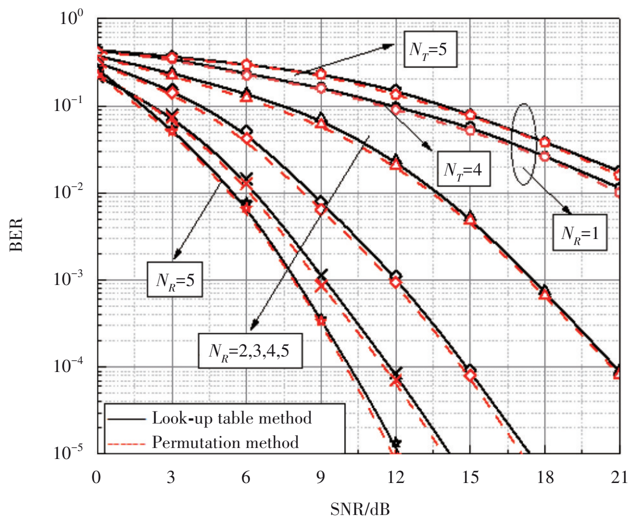

BER: bit error rate SNR: signal-to-noise ratio

▲ **Figure 2. BER performance of DSM with Permutation Method (PM) and Look-Up Table Order (LUTO) with BPSK modulation**

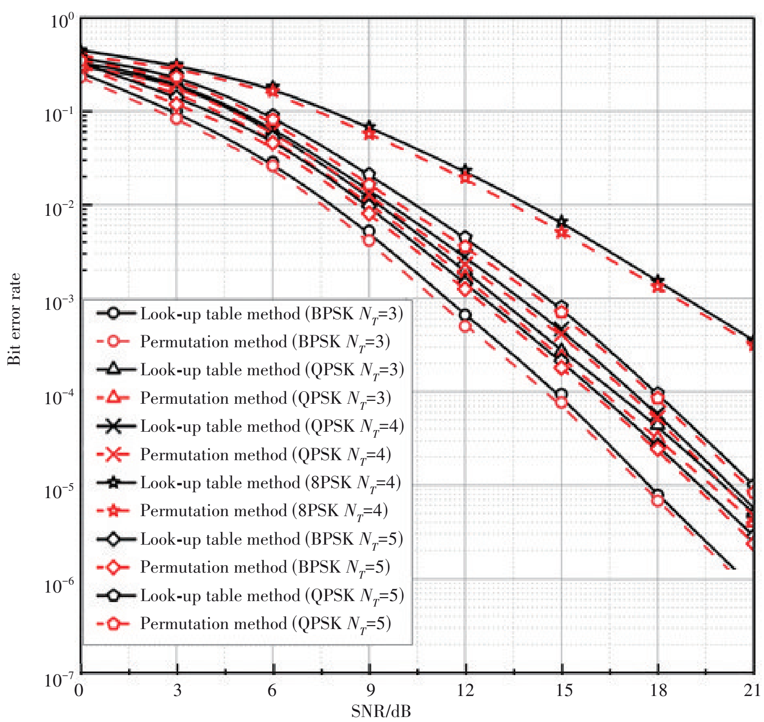

8PSK: 8 Phase shift keying QPSK: quadrature phase shift keying
BPSK: binary phase shift keying SNR: signal-to-noise ratio

▲ **Figure 3. Simulation and theoretical results of the system with different modulation for different differential spatial modulation (DSM) with N_R = 3**

6 Conclusions

In this paper, the design of DSM's mapping algorithms, LUTO and PM, particularly when used with a high number of antennas, is further expanded upon. A detailed description and performance analysis of these two mapping algorithms are presented. Simulation results show that the PM algorithm is slightly better than the LUTO algorithm in terms of BER, although its implementation is more complicated. The LUTO algorithm, on the other hand, is relatively simple but requires additional lookup table storage space. The selection of the appropriate method should be based on the specific situation.

References

[1] DI RENZO M, HAAS H, GRANT P M. Spatial modulation for multiple-antenna wireless systems: A survey [J]. IEEE communications magazine, 2011, 49(12): 182 – 191. DOI: 10.1109/MCOM.2011.6094024
[2] MESLEH R Y, HAAS H, SINANOVIC S, et al. Spatial modulation [J]. IEEE transactions on vehicular technology, 2008, 57(4): 2228 – 2241. DOI: 10.1109/TVT.2007.912136
[3] WEN M W, ZHENG B X, KIM K J, et al. A survey on spatial modulation in emerging wireless systems: Research progresses and applications [J]. IEEE journal on selected areas in communications, 2019, 37(9): 1949 – 1972. DOI: 10.1109/JSAC.2019.2929453
[4] LI J, DANG S P, WEN M W, et al. Index modulation multiple access for 6G communications: Principles, applications, and challenges [J]. IEEE network, 2023, 37(1): 52 – 60. DOI: 10.1109/MNET.002.2200433
[5] LI J, DANG S P, YAN Y E, et al. Generalized quadrature spatial modulation and its application to vehicular networks with NOMA [J]. IEEE transactions on intelligent transportation systems, 2021, 22(7): 4030 – 4039. DOI: 10.1109/TITS.2020.3006482
[6] LI J, DANG S P, HUANG Y, et al. Composite multiple-mode orthogonal frequency division multiplexing with index modulation [J]. IEEE transactions on wireless communications, 2023, 22(6): 3748 – 3761. DOI: 10.1109/TWC.2022.3220752
[7] WEN M W, LI J, DANG S P, et al. Joint-mapping orthogonal frequency division multiplexing with subcarrier number modulation [J]. IEEE transactions on communications, 2021, 69(7): 4306 – 4318. DOI: 10.1109/TCOMM.2021.3066584
[8] WEN M W, LIN S E, KIM K J, et al. Cyclic delay diversity with index modulation for green Internet of Things [J]. IEEE transactions on green communications and networking, 2021, 5(2): 600 – 610. DOI: 10.1109/TGCN.2021.3067705
[9] WEN M W, CHEN X, LI Q, et al. Index modulation aided subcarrier mapping for dual-hop OFDM relaying [J]. IEEE transactions on communications, 2019, 67(9): 6012 – 6024. DOI: 10.1109/TCOMM.2019.2920642
[10] JEGANATHAN J, GHRAYEB A, SZCZECINSKI L. Spatial modulation: optimal detection and performance analysis [J]. IEEE communications letters, 2008, 12(8): 545 – 547. DOI: 10.1109/LCOMM.2008.080739
[11] BIAN Y Y, WEN M W, CHENG X, et al. A differential scheme for Spatial Modulation [C]//Proc. IEEE Global Communications Conference (GLOBECOM). IEEE, 2013: 3925 – 3930. DOI: 10.1109/GLOCOM.2013.6831686
[12] ISHIKAWA N, SUGIURA S. Unified differential spatial modulation [J]. IEEE wireless communications letters, 2014, 3(4): 337 – 340. DOI: 10.1109/LWC.2014.2315635

[13] BIAN Y Y, CHENG X, WEN M W, et al. Differential spatial modulation [J]. IEEE transactions on vehicular technology, 2015, 64(7): 3262 – 3268. DOI: 10.1109/TVT.2014.2348791

[14] LI J, WEN M W, CHENG X, et al. Differential spatial modulation with gray coded antenna activation order [J]. IEEE communications letters, 2016, 20(6): 1100 – 1103. DOI: 10.1109/LCOMM.2016.2557801

[15] ZHANG M, WEN M W, CHENG X, et al. A dual-hop virtual MIMO architecture based on hybrid differential spatial modulation [J]. IEEE transactions on wireless communications, 2016, 15(9): 6356 – 6370. DOI: 10.1109/TWC.2016.2583423

[16] RAJASHEKAR R, XU C, ISHIKAWA N, et al. Algebraic differential spatial modulation is capable of approaching the performance of its coherent counterpart [J]. IEEE transactions on communications, 2017, 65(10): 4260 – 4273. DOI: 10.1109/TCOMM.2017.2720170

[17] XU C, WANG L, NG S X, et al. Soft-decision multiple-symbol differential sphere detection and decision-feedback differential detection for differential QAM dispensing with channel estimation in the face of rapidly fading channels [J]. IEEE transactions on wireless communications, 2016, 15(6): 4408 – 4425. DOI: 10.1109/TWC.2016.2541665

[18] WEI R Y, TSAI Y W, CHEN S L. Improved schemes of differential spatial modulation [J]. IEEE access, 2021, 9: 97120 – 97128. DOI: 10.1109/ACCESS.2021.3095531

[19] WEN M W, CHENG X, BIAN Y Y, et al. A low-complexity near-ML differential spatial modulation detector [J]. IEEE signal processing letters, 2015, 22(11): 1834 – 1838. DOI: 10.1109/LSP.2015.2425042

[20] WEI R Y, CHEN S L, LIN Y H, et al. Bandwidth-efficient generalized differential spatial modulation [J]. IEEE transactions on vehicular technology, 2023, 72(1): 601 – 610. DOI: 10.1109/TVT.2022.3202912

[21] XIU H T, YU D Z, GAO P Y, et al. An enhanced system model for differential spatial modulation system under fast fading channels and a corresponding DFDD based low- complexity detector [J]. IEEE transactions on vehicular technology, 2024, 73(2): 2227 – 2235. DOI: 10.1109/TVT.2023.3316275

[22] YANG L, XIU H T, YU D Z, et al. Reordered amplitude phase shift keying aided differential spatial modulation: DFDD-based low-complexity detector and performance analysis over fading channels [J]. IEEE transactions on wireless communications, 2022, 21(10): 7913 – 7925. DOI: 10.1109/TWC.2022.3162834

[23] WEI R Y. Differential encoding by a look-up table for quadrature-amplitude modulation [J]. IEEE transactions on communications, 2011, 59(1): 84 – 94. DOI: 10.1109/TCOMM.2010.102910.100061

Biographies

WANG Chanfei (wangchanfei@163.com) received her MS degree in communication and information systems from Lanzhou University of Technology, China in 2008 and PhD degree from Beijing University of Posts and Telecommunications (BUPT), China in 2016. She is currently an associate professor and a master's degree supervisor with the College of Computer and Communication, Lanzhou University of Technology. Her research interest is signal detection in communication system.

CHAI Jianxin is currently pursuing his master's degree in the Department of Communication Engineering, Lanzhou University of Technology, China. His research interests include differential spatial modulation andsignal detection and estimation.

XU Yamei received her PhD degree from Xidian University, China. She is currently an associate professor and the master's degree supervisor with the College of Computer and Communication, Lanzhou University of Technology, China. Her research interest is pattern recognition.